JOC The Journal of Organic Chemistry

pubs.acs.org/joc Article

Spacer-Mediated Control of Coumarin Uncaging for Photocaged Thymidine

Shengzhuang Tang, Jayme Cannon, Kelly Yang, Matthew F. Krummel, James R. Baker, Jr., and Seok Ki Choi*

Cite This: https://dx.doi.org/10.1021/acs.joc.9b02617 Read Online

ACCESS | Metrics & More | Article Recommendations | Supporting Information

ABSTRACT: Despite its importance in the design of photocaged molecules, less attention is focused on linker chemistry than the cage itself. Here, we describe unique uncaging properties displayed by two coumarin-caged thymidine compounds, each conjugated with (**2**) or without (**1**) an extended, self-immolative spacer. Photolysis of **1** using long-wavelength UVA (365 nm) or visible (420, 455 nm) light led to the release of free thymidine along with the competitive generation of a thymidine-bearing recombination product. The occurrence of this undesired side reaction, which is previously unreported, was not present with the photolysis of **2**, which released thymidine exclusively with higher quantum efficiency. We propose that the spatial separation between the cage and the substrate molecule conferred by the extended linker can play a critical role in circumventing this unproductive reaction. This report reinforces the importance of linker selection in the design of coumarin-caged oligonucleosides and other conjugates.

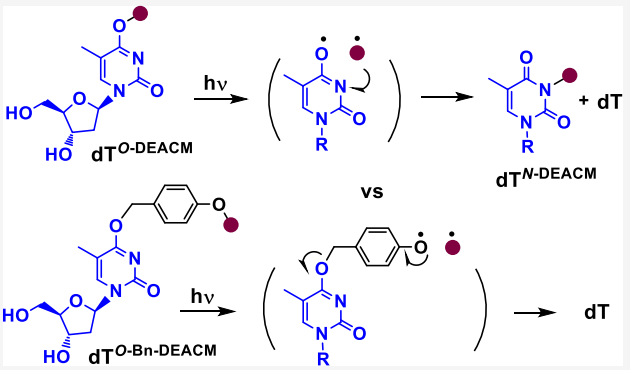

INTRODUCTION

Photocaging refers to temporarily conjugating a functional molecule with a photocleavable group[1] as a strategy to prevent its activity until temporally or spatially released by light.[2−5] Since its first application to neurotransmitter ligands for channel gating studies including those by Hoffman et al.[2] and Hess et al.,[3] photocaging applications have expanded to various fields including cellular signaling,[6−9] imaging,[10,11] optogenetics,[12−15] photopharmacology,[16,17] and drug delivery.[11,18−20] This strategy also plays a key role in the design of oligonucleotide probes that enable light-controlled DNA hybridization[21−24] and gene regulation.[25,26]

The efficiency of photon-mediated release of caged drugs or biomolecules is largely dependent on the cage moiety because this chromophore directly determines the wavelength selectivity and mechanism associated with the release.[1,27,28] However, the cage structure can also be responsible for the occurrence of undesired recombination reactions[12,29,30] that can reduce the uncaging efficiency. In this current study, we examine the concept that linker optimization can enhance the uncaging efficiency while circumventing undesired side reactions. We illustrate this concept using coumarin-caged thymidine (Figure 1), the type of structure frequently used in the synthesis of photocaged oligonucleotides.[1,28,31]

Various cage molecules have been developed, which include *ortho*-nitrobenzene,[3,32−34] coumarin,[1,10,28,35,36] carbazole,[37,38] and quinoline.[39−42] Some of these are used for thymidine photocaging including coumarin,[23,24,43,44] *ortho*-nitrobenzene,[24,45−47] and *p*-hydroxyphenylacyl.[24,48] Of these, coumarin displays distinct structural and photochemical properties.[1,10,28,35,36] It shows several benefits such as high molar absorptivity in the UV and visible light (320−440 nm), use for wavelength-selective uncaging,[6,24,28,29,49] and ability for two-photon uncaging at the near-infrared wavelength (720 and 830 nm).[7] Its flexible linkage chemistry at the C4 position allows photocaging applications to a variety of substrates containing functional moieties of carboxylate,[10] amide,[50] amine,[51] alcohol,[12,52,53] thiol,[29,54] and phosphate.[36,55,56] It also serves as an effective protecting group for the carbonyl functionality of a nucleotide base as in the synthesis of caged 2′-deoxyguanosine[22] and 2′-deoxythymidine.[23,24] Access to such caged compounds has led to diverse applications in biological and biomedical areas by enabling spatiotemporal control in fluorescence imaging,[10,56] mapping of ligand-evoked channel gating,[6,7,10] therapeutic activation or delivery,[51,57] signal transduction,[6,52,54,56] DNA hybridization,[22−24] and gene expression.[12,25]

Received: September 26, 2019

https://dx.doi.org/10.1021/acs.joc.9b02617
J. Org. Chem. XXXX, XXX, XXX−XXX

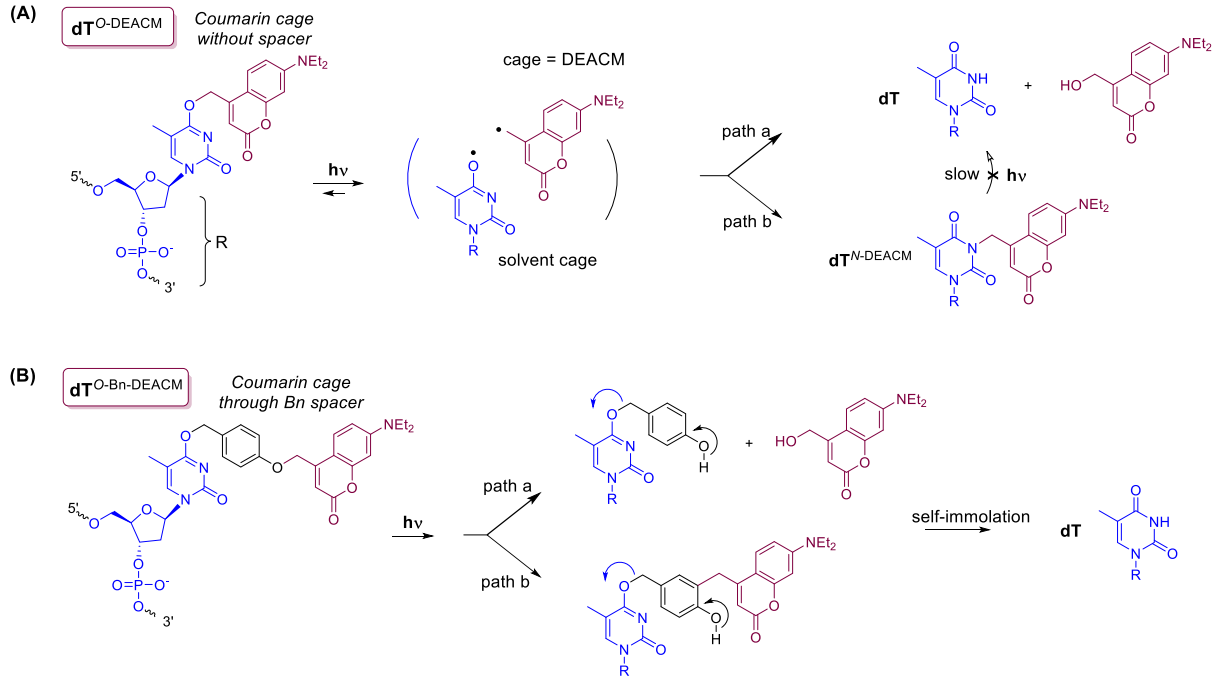

Figure 1. Competing paths proposed in the radical-based photon uncaging of thymidine (**dT**) caged with coumarin through no spacer (A) or a self-immolative benzyl (Bn) spacer (B). DEACM = 7-diethylamino-4-methylcoumarin.

Scheme 1. Synthesis of Coumarin-Caged Thymidines 1 and 2[a]

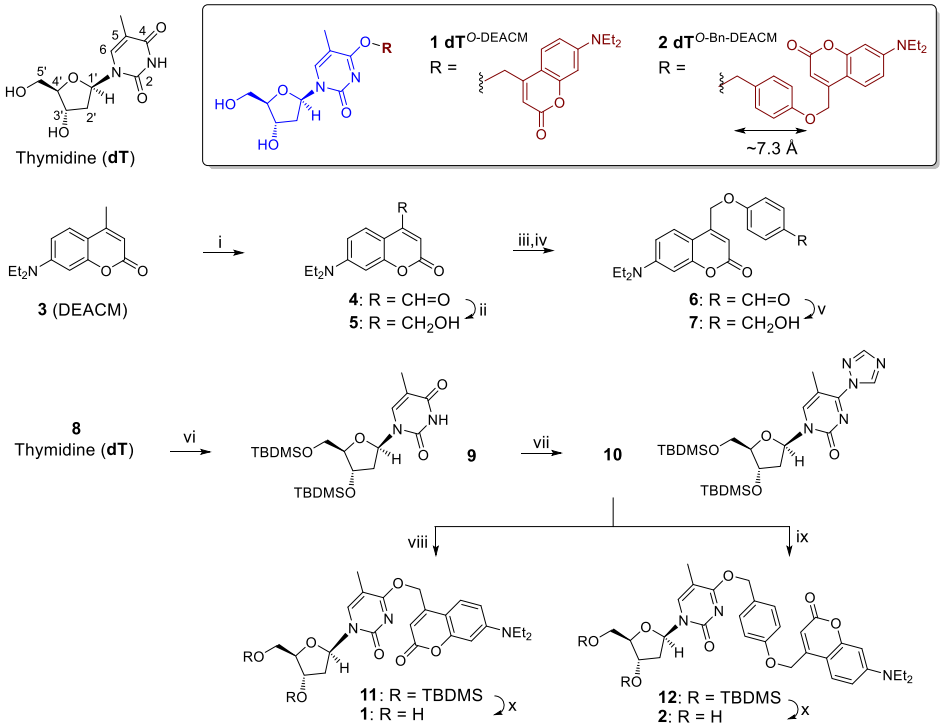

[a]Reagents and conditions: (i) SeO_2, xylene, 150 °C; (ii) $NaBH_4$, MeOH, 0 °C to rt; (iii) MsCl, Et_3N, CH_2Cl_2, 0 °C; (iv) 4-hydroxybenzaldehyde, K_2CO_3, THF, 45 °C, 60%; (v) $NaBH_4$, MeOH, rt, 84%; (vi) *tert*-butyldimethylsilyl chloride (TBDMS-Cl), imidazole, DMF, 100%; (vii) $POCl_3$, 1,2,4-1*H*-triazole, MeCN, 0 °C, 85%; (viii) **5**, 1,8-diazabicyclo[5.4.0]undec-7-ene (DBU), MeCN, rt, 97%; (ix) **7**, DBU, MeCN, rt, 93%; (x) Bu_4NF, AcOH, THF, rt, 82% (for **1**), 71% (for **2**).

Compared to *ortho*-nitrobenzene uncaging which occurs selectively via an intramolecular cyclization,[1,58] coumarin uncaging occurs via a homolytic and/or heterolytic bond cleavage.[27] Therefore, it involves the generation of a transient radical (or ion) pair, which remains reactive (Figure 1). However, because of their close spatial proximity, the radical pair has the potential to undergo an undesired recombination reaction (path b) via [1,3] photoisomerization (or more broadly defined photo-Claisen rearrangement[59]) in lieu of the release of an uncaged molecule (path a). Recently, a few

https://dx.doi.org/10.1021/acs.joc.9b02617
J. Org. Chem. XXXX, XXX, XXX−XXX

studies[29,30,60−62] including ours[12] reported the occurrence of undesired side products in the photolysis of quinoline-caged tertiary amines,[61,62] coumarin-caged peptides,[29,30] capsaicin,[60] and 4-hydroxytamoxifen.[12] While the prevalence of these side reactions varies with the structure and linkage type of an individual caged molecule, we demonstrated that the spatial separation of the coumarin cage through an extended spacer prevents these side reactions, thus enhancing the uncaging efficiency.[12]

In the present study, we investigate the occurrence of undesired photo-catalyzed rearrangement in a coumarin ether-caged thymidine and develop linker chemistry for blocking these side reactions. First, we describe linker chemistries for the synthesis of two thymidine (**dT**)-caged compounds (Figure 1). The first utilizes a standard approach based on a direct ether linkage.[22−24] The second involves a novel approach based on a 4-hydroxybenzyl spacer, which was selected because it appeared to provide sufficient length for spatial separation of the radical (or ion) pair as well as to facilitate the self-immolative release[63] of thymidine even from the undesired byproduct (path b). We also present evidence for the central role of these linker designs in determining the release kinetics of free thymidine by irradiation at either UV (365 nm) or visible light (420, 455 nm). This information provides novel insights that help advance our understanding of the role of linker chemistry in the photoactivation of caged molecules.

RESULTS AND DISCUSSION

Synthesis of Coumarin Cages. Scheme 1 summarizes the synthesis of two coumarin cages, which include 7-diethylaminocoumarin-4-methyl (DEACM) alcohol (**5**)[36] and **7**. Coumarin cage **5** was synthesized according to literature protocols that involve selenium dioxide[12,36,64] oxidation of **3** to an aldehyde derivative **4** and subsequent reduction to **5** using sodium borohydride.[12,36] In our previous approach on linker extension for **5**,[12] we employed a carbamate-based linkage through N^1,N^2-dimethylethane-1,2-diamine as the self-immolative spacer. However, this approach has not been applicable for thymidine because of the lack of synthetic methodology developed for the carbamate linkage at its O-4 position, the preferred site for photocaging. Therefore, we designed a new approach by derivatizing **5** to **7** for use as an ether-based self-immolative linker, which is compatible at O-4.

Compound **7** is a new structure with a 4-hydroxybenzyl spacer attached at its phenolic moiety to DEACM through an ether linkage. Its end-to-end length (~7.3 Å), which is predicted in a stable extended conformation, is similar to the distance (~6.8 Å) of a spacer (N^1,N^2-dimethylethane-1,2-diamine) that was shown to be effective in preventing the undesired photo-Claisen rearrangement that occurs during coumarin release.[12] The synthesis of **7** was performed in two steps: (i) O-alkylation of 4-hydroxybenzaldehyde with the *O*-methanesulfonate[12] derivative of **5** and (ii) sodium borohydride reduction of the aldehyde to a hydroxymethyl derivative. Its structural identity is consistent with the data from standard analytical methods including high-resolution mass spectrometry (HRMS), showing agreement of the observed molecular mass with the calculated theoretical value for **7** ($C_{21}H_{21}NO_4$ $[M + H]^+$, 352.1549; found, 352.1544).

Synthesis of Coumarin-Caged Thymidines. The synthesis of each caged thymidine **1**[23] and **2** was performed using a conventional strategy long established for nucleoside bases. This involves the nucleophilic reaction of each cage molecule with triazolyl thymidine,[65,66] resulting in an O-substitution at the 4 position (Scheme 1). First, thymidine (**dT**) was fully protected as *O*-TBDMS **9** and converted to triazolylpyrimidinone **10** according to the established protocol.[65,66] Its structure is in agreement with NMR data and HRMS (ESI) calculated for **10** ($C_{24}H_{43}N_5O_4Si_2$ $[M + H]^+$, 522.2932; found, 522.2927, Figure S4).

Compound **1** $\mathbf{dT}^{\mathbf{O\text{-}DEACM}}$ was prepared in two steps that began with the O-substitution of **10** with a coumarin cage **5** under a condition catalyzed by DBU. This led to **11** (93%; HRMS calcd for $C_{36}H_{57}N_3O_7Si_2$ $[M + H]^+$, 700.3813; found, 700.3806), and its *O*-TBDMS was deprotected by treatment with tetrabutylammonium fluoride (TBAF)/acetic acid in tetrahydrofuran (THF), affording **1** (isolated yield 82%). It was characterized for its structural identity by NMR (^{1}H, ^{13}C) spectroscopy, HRMS (calcd for $C_{24}H_{29}N_3O_7$ $[M + Na]^+$, 494.1903; found, 494.1898), and UV−vis spectrophotometry (Figure 2). Its characterization data are fully consistent with

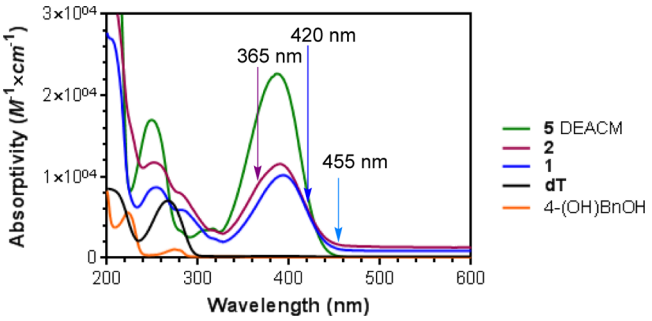

Figure 2. UV−vis absorption spectra of caged thymidine compounds **1**, **2** and their building blocks. Each arrow indicates the relative level of absorption at the wavelength of light used in uncaging experiments.

the anticipated values as reported in the literature.[23] Its purity was determined as ≥95% by ultraperformance liquid chromatography (UPLC) (Figure S12, Supporting Information).

Compound **2** $\mathbf{dT}^{\mathbf{O\text{-}Bn\text{-}DEACM}}$ was prepared in the same manner as for **1** except replacing **5** with **7**. Its synthesis involved O-substitution of **10** with a coumarin cage **7** under the conditions catalyzed by DBU, leading to **12** (97%; HRMS calcd for $C_{43}H_{64}N_3O_8Si_2$ $[M + H]^+$, 806.4232; found, 806.4223). The caged thymidine **2** was obtained upon deprotection of *O*-TBDMS **12** by treatment with TBAF/acetic acid in THF (isolated yield 71%). Its structural identity was fully characterized by NMR (^{1}H, ^{13}C) spectroscopy (Figure S9), MS, and UV−vis spectrophotometry (Figure 2). Its exact molecular mass is in good agreement with an experimental value measured by HRMS (calcd for $C_{21}H_{35}N_3O_8$ $[M + H]^+$, 578.2502; found, 578.2496). Its purity was ≥95% by UPLC analysis (Figure S12).

UV−Vis Absorption Property. We observed the absorption properties of the coumarin (DEACM), a common cage present in **1** and **2**, as shown in their UV−vis spectra (Figure 2). It shows a broad range of strong absorption (340−440 nm) with λ_{max} values at 393 nm (**1**, ε = 10,209 M^{-1} cm^{-1}) and 390 nm (**2**, ε = 11,603 M^{-1} cm^{-1}), which remain almost unchanged compared to the absorption of the cage alone (λ_{max} = 387 nm, ε = 22,687 M^{-1} cm^{-1}). We selected three different wavelengths for investigating uncaging kinetics of **1** and **2**, which include 365 nm (long-wavelength UVA) and 420 nm

https://dx.doi.org/10.1021/acs.joc.9b02617
J. Org. Chem. XXXX, XXX, XXX−XXX

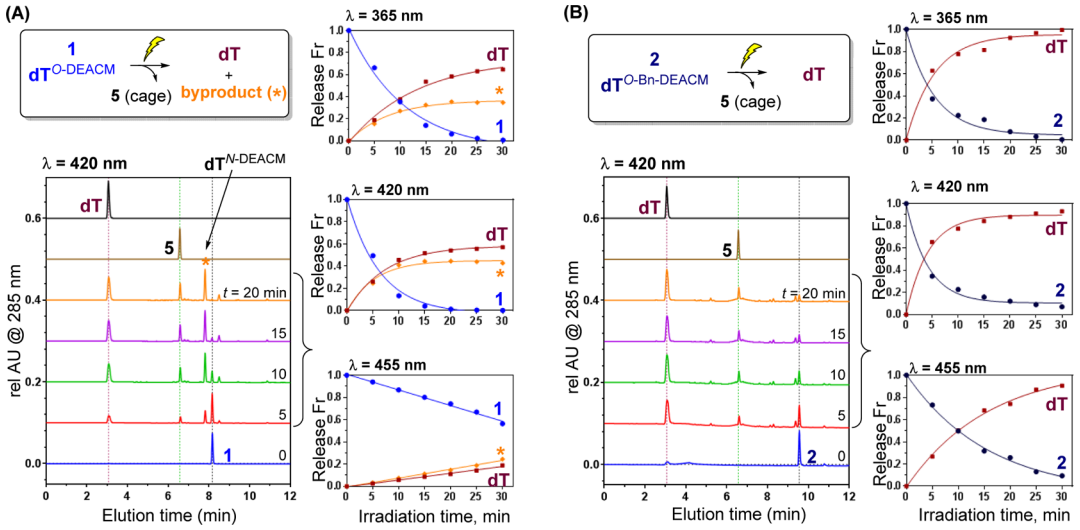

Figure 3. Uncaging kinetics of **1** (A) and **2** (B) by photolysis using long-wavelength UV (365 nm) or visible light (420, 455 nm). Representative UPLC traces (left) refer to those at 420 nm acquired after the indicated period of photolysis of **1** and **2**, respectively, at 0.1 mg/mL in 35% (v/v) aq methanol. Each plot (right) shows the fraction (Fr) of thymidine (**dT**) and a byproduct (*; **dT**$^{N\text{-DEACM}}$) released as a function of irradiation time. Each Fr is based on % area under curve (AUC) analysis of the released products from UPLC traces.

Table 1. Summary of Photouncaging Efficiency of Coumarin-Caged Thymidine Compounds

	365 nm			420 nm			455 nm		
		Φ[b]			Φ[b]			Φ[b]	
caged thymidine	k_{decay} (s^{-1})[a]	**dT**	byproduct	k_{decay} (s^{-1})[a]	**dT**	byproduct	k_{decay} (s^{-1})[a]	**dT**	byproduct
1 dT$^{O\text{-DEACM}}$	8.9×10^{-4}	0.006	0.005	1.5×10^{-3}	0.015	0.017	1.2×10^{-4}	0.017	0.023
2 dT$^{O\text{-Bn-DEACM}}$	1.1×10^{-3}	0.014		1.1×10^{-3}	0.025		5.8×10^{-4}	0.081	

[a]Rate constant (first order) for the decay of caged thymidine **1** or **2**. [b]Quantum efficiency (Φ) of release for thymidine (**dT**) or thymidine-retaining byproduct **dT**$^{N\text{-DEACM}}$ = $[dc/dt]_{initial}/[q_{n,p}(1 - 10^{-A})]$, where $q_{n,p}$ = photon flux (q_p/N_A, mol s^{-1}) measured by ferrioxalate actinometry.[67,68] dc/dt = initial rate of thymidine or byproduct release (mol s^{-1}). A = absorbance of **1** or **2** at the wavelength of irradiated light.

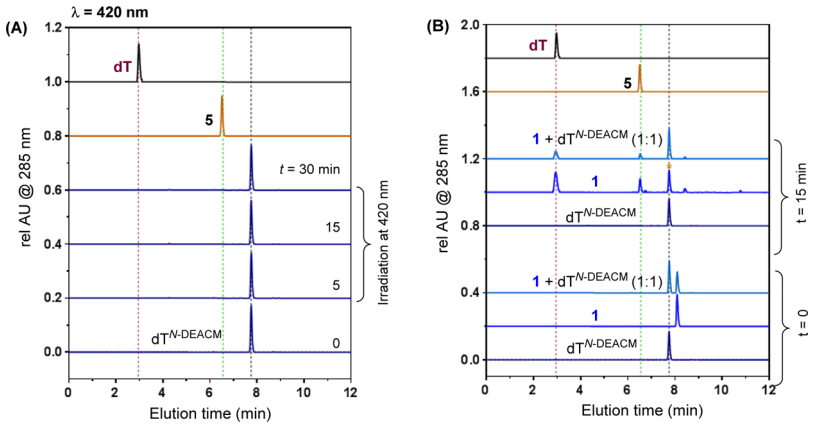

Figure 4. Uncaging kinetics of **dT**$^{N\text{-DEACM}}$ by photolysis at 420 nm. (A) Representative UPLC traces overlaid and (B) comparison with the traces of **1** dT$^{O\text{-DEACM}}$. Each of the traces labeled as **1** + **dT**$^{N\text{-DEACM}}$ (B) refers to the coinjection (1:1 mixture) of two indicated samples, each prepared separately. Their photolysis was performed as described in Figure 3.

(visible light) as the preferred range and 455 nm as a comparator that appears less effective for photoactivation given weaker molar absorptivity (ε = 1115 (**1**) or 1653 (**2**) M^{-1} cm^{-1}). The benzyl spacer present in **2** lacks any absorbance above 300 nm, and it has no effect on the photoactivation at any of these wavelengths.

Uncaging Kinetics via Direct Ether Linkage. Photolysis of **1** was performed in an aqueous medium (0.21 mM) supplemented with methanol (35%, v/v) for improving its poor aqueous solubility, and its release kinetics was determined by monitoring exposed solutions using UV−vis spectroscopy and UPLC (Figure 3). UV−vis spectra acquired after photolysis at 420 nm (exposure time = 0−20 min) show absorption changes in an exposure and time-dependent manner (Figure S13), but these are not adequate for the detection and quantitation of thymidine released. In contrast, UPLC traces acquired after photolysis (Figure 3A) show the disappearance of **1** with the concomitant growth of free thymidine (**dT**) (t_r = 3.1 min) along with coumarin cage released **5** (t_r = 6.5 min). The AUC analysis of these peaks

https://dx.doi.org/10.1021/acs.joc.9b02617
J. Org. Chem. XXXX, XXX, XXX−XXX

Scheme 2. Synthesis of dT$^{O\text{-Bn-DEACM}}$ 2 Phosphoramidite[a]

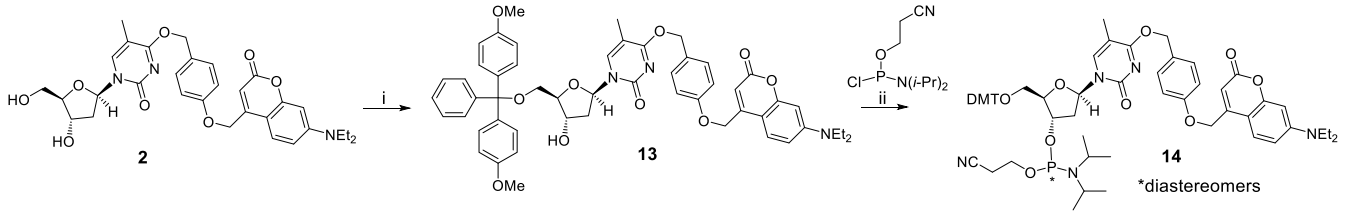

[a]Reagents and conditions: (i) dimethoxytrityl chloride (DMT-Cl), pyridine, 61% and(ii) *N*,*N*-diisopropyl-*N*-ethylamine (DIPEA), dichloromethane, 73%.

provided a decay curve for compound **1** (right, Figure 3A). Its regression analysis demonstrated a rate constant for first-order decay (k_{decay} = 1.5 × 10^{-3} s^{-1}), quantum efficiency (Φ_{dT} = 0.015), and sensitivity ($\Phi_{dT} \times \varepsilon$ = 108 M^{-1} cm^{-1}) for thymidine release (Tables 1 and S1).

It is important to note that the UPLC traces also indicate the release of an unknown species (t_r = 7.8 min) that grows during exposure in a time-dependent manner. It accounts for a significant fraction in terms of quantum efficiency ($\Phi_{byproduct}$ = 0.017) compared to free thymidine. In order to characterize the unknown product, the photolysis continued up to 30 min until **1** was fully consumed, and this exposed solution was analyzed by HPLC−MS (Figure S15). The peak assigned to the unknown species shows no difference in its molecular mass (found 472.2082) relative to **1** (calcd for $[M + H]^+$ = 472.2084).

We cautiously assigned this byproduct as a thymidine-bearing **dT$^{N\text{-DEACM}}$** and verified its identity by its independent synthesis and characterization by ^{1}H NMR, HRMS (Figure S7), and UPLC (Figure S12), collectively supportive of its N-isomeric relationship to **1**. We hypothesize that it might result from the recombination of the two detached species (i.e., a coumarin and thymidine radical pair), which are retained in close proximity in a solvent cage, via O- to N-photoisomerization or [1,3] photo-Claisen rearrangement,[59,69] as depicted in Figure 1A (path b). Once generated, this **dT$^{N\text{-DEACM}}$** practically loses its ability for photon uncaging because it remains stable even after sufficiently long irradiation (420 nm, 30 min) as indicated by UPLC traces (Figure 4A). Its lack of uncaging is consistent, in part, with a report that an oligonucleotide containing **dT$^{N\text{-DEACM}}$** decays approximately 2 orders of magnitude more slowly than an equivalent oligonucleotide containing **1 dT$^{O\text{-DEACM}}$**.[23] In addition, its UPLC traces confirm that it is identical to the byproduct released from **1** (Figure 4B).

We also performed the photolysis of **1** at two other wavelengths (365, 455 nm) to determine whether the occurrence of such an undesired product is dependent on light wavelength. Photolysis at 365 nm occurred at a rate similar to 420 nm and showed a comparable decay rate (k_{decay} = 8.9 × 10^{-4} s^{-1}). It also displayed a similar pattern of product distribution that includes the undesired product (Figure S14A). Photolysis at 455 nm occurred 7−13-fold more slowly (k_{decay} = 1.2 × 10^{-4} s^{-1}) than at either 365 or 420 nm, respectively (Table 1). Its photolysis products also included the undesired species **dT$^{N\text{-DEACM}}$** ($\Phi_{byproduct}$ = 0.023) in addition to thymidine. Thus, although the wavelength of light plays a role in determining the rate of decay, it does not alter the distribution of the released products. In summary, the photolysis of **1** produced a thymidine-bearing byproduct, perhaps because of the direct ether linkage of coumarin to thymidine.

Uncaging Kinetics via the Extended Spacer. We similarly evaluated the uncaging kinetics of **2 dT$^{O\text{-Bn-DEACM}}$** (0.17 mM in 35% (v/v) aq methanol) by irradiation at 420 nm (Figure 3B). Its photolysis led to smaller changes in UV−vis spectra with the lack of a clear trend compared to **1 dT$^{O\text{-DEACM}}$** (Figure S13). Overlaid UPLC traces show time-dependent, rapid uncaging of **2** with ∼65% release of thymidine achieved after an initial exposure for only 5 min. However, we did not observe the undesired species (t_r = 7.8 min) from the photolysis of **2** that was seen with **1**. Regression analysis of its decay curve provided a decay constant (k_{decay} = 1.1 × 10^{-3} s^{-1}), which is slightly lower than that of **1** (Table 1). However, its lack of byproduct formation enhances its quantum efficiency and sensitivity for thymidine release (Φ_{dT} = 0.025, $\Phi_{dT} \times \varepsilon$ = 183 M^{-1} cm^{-1}) compared to **1** (Φ_{dT} = 0.015, $\Phi_{dT} \times \varepsilon$ = 108 M^{-1} cm^{-1}). The single product and efficient kinetics demonstrated with compound **2** offer evidence of advantages in thymidine release from a cage with an extended linker as compared to the direct ether linkage.

Similarly, photolysis of **2** was studied at 365 and 455 nm. Photolysis at 365 nm occurred as rapidly as at 420 nm without the release of the byproduct (Figure S14B). It led to greater quantum efficiency for thymidine release (Φ_{dT} = 0.014) than **1** (Φ_{dT} = 0.006) under an identical condition (365 nm). Photolysis at 455 nm provided a similar result (Figure S14B), although it occurred at a rate approximately 2-fold lower than at 420 nm. This slower decay is anticipated given lower molar absorptivity at 455 nm (Figure 2). However, it is notable that **2** showed ∼5-fold faster decay than **1** at 455 nm (Table 1). This suggests that the spatial separation conferred by the extended spacer might be able to prevent an unwanted recombination event involving the detached species back to the parent **2** as well (Figure 1).

Synthesis of dT$^{O\text{-Bn-DEACM}}$ Phosphoramidite. The new caged thymidine **2** offers potential utility as a building block in oligonucleotide synthesis. As summarized in Scheme 2, it is readily applicable for use with a standard nucleoside chemistry involved in the synthesis of DMT-protected phosphoramidite. As fully detailed in the Experimental Section, **2** was converted to its phosphoramidite **14** in two steps (overall 45%). These include the regiospecific protection of its hydroxymethyl group at C5 with DMT (**13**) and a subsequent derivatization to **14** phosphoramidite at C4.

In summary, we quantitatively measured the decay rate and quantum efficiency of thymidine release from coumarin-caged thymidine prepared via either a direct ether linkage or an extended linker with a self-immolative spacer.[63] The direct linkage in **1 dT$^{O\text{-DEACM}}$** allows a fast decay upon activation with either visible (420 nm) or long-wavelength UVA (365 nm)

https://dx.doi.org/10.1021/acs.joc.9b02617
J. Org. Chem. XXXX, XXX, XXX−XXX

irradiation. However, it induces a thymidine-bearing byproduct $dT^{N\text{-}DEACM}$ regardless of the light wavelength used. In contrast, the presence of the extended spacer in **2** $dT^{O\text{-}Bn\text{-}DEACM}$ leads to better results including a fast decay, lack of the byproduct formed, and greater efficiency of thymidine release (max 94 vs 58% with compound **1**). We also demonstrated the synthesis of **14** phosphoramidite, a new caged building block applicable to the synthesis of caged oligonucleotides.

CONCLUSIONS

This study offers a number of insights that advance our knowledge in the use of photocaging. First, it offers evidence for the presence of photorearrangement[59,69] in coumarin ether-caged thymidine **1**, with the side reaction reported here being identified for the first time. Thus, this study adds another example of photorearrangement to a growing list of substrates where this phenomenon is observed.[29,30,60] Second, this study highlights the importance of validating the release efficiency using an isolated caged unit because it is better suited for accurate and sensitive analysis than when it is present in oligomeric units or coupled to larger macromolecules. Here, we were able to determine uncaging kinetics by testing a caged thymidine instead of a caged oligonucleotide,[21−24,53] while photolysis analysis of the latter by HPLC[21−24,53] appears to be unable to detect structural alterations that could occur after uncaging or rearrangement. Third, this study highlights the importance of developing an optimal analytical method for monitoring these structures, such as UPLC. Other methods commonly employed for evaluating uncaging kinetics, such as UV−vis spectrometry (Figure S13) and thin-layer chromatography (TLC),[12] lack sufficient product separation with high resolution.

Photocaging continues to increase in popularity for light-controlled activation and has been applied to an increasing variety of substrates ranging from small-molecule ligands,[3,7,10] therapeutic agents,[12,19,33] peptides,[29,30,32] proteins[9] to oligonucleotides.[22−24] Factors important for controlling the uncaging efficiency include light wavelength,[6,10,28,43] exposure time, and media pH[58] as well as the type of the cage molecule.[12,24,34,38] Here, we present evidence that linker chemistry also plays an important role in determining the uncaging efficiency for certain cage types such as coumarin. Importantly, this result is consistent with recent findings performed with other classes of substrates based on thiols and phenols.[12,29,30] In summary, this study validates using a hydroxy benzyl spacer strategy for preventing coumarin recombination, which can be potentially applicable to a broad range of substrates from nucleotides (cytidine,[70] guanosine[22]) to therapeutic molecules including those tested for light-controlled prodrug activation.[12,71−73]

EXPERIMENTAL SECTION

Materials and Methods. Unless otherwise noted, all reagents and solvents were used as received from commercial suppliers. These include thymidine (≥99%), 4-hydroxybenzaldehyde (98%), methanesulfonyl chloride (99.7%), 2-cyanoethyl *N*,*N*-diisopropylchlorophosphoramidite, 4,4′-dimethoxytriphenylmethyl chloride (≥97%), acetonitrile, dichloromethane, cyclohexanes, hexanes, and ethyl acetate (all from Sigma-Aldrich), 7-(diethylamino)-4-methyl-2*H*-chromen-2-one (98%, TCI America), *tert*-butyldimethylchlorosilane (97%, Alfa Aesar), and 1,2,4-1*H*-triazole (99.5%, Acros Organics).

^{1}H and ^{13}C NMR spectral data were acquired in deuterium-labeled solvents including $CDCl_3$ (99.96% D), DMSO-d_6 (99.9% D), CD_3OD (99.8% D), and D_2O (99.9% D), each purchased from Cambridge Isotope Laboratories, Inc. Column chromatography was performed using silica gel of 200−400 mesh, and TLC was performed with silica plates with a 250 μm thickness (Merck).

Analytical Methods. Caged products and their intermediates were characterized for their structural identity and homogeneity by standard analytical methods including NMR (^{1}H, ^{13}C) spectroscopy, HRMS, UV−vis spectrometry, and UPLC.[12]

NMR spectra were acquired using a spectrometer from Varian (500 MHz for ^{1}H; 100 MHz for proton-decoupled ^{13}C) at 297.3 K using a standard default pulse sequence. Chemical shift values for ^{1}H NMR spectra are reported in parts per million relative to tetramethylsilane (TMS) or sodium 2,2-dimethyl-2-silapentane-5-sulfonate, each serving as an internal standard (δ = 0.00 ppm), or relative to known residual signals from the deuterated solvent used.

Mass spectral data were acquired using a Micromass AutoSpec Ultima Magnetic sector mass spectrometer in an electrospray ionization (ESI) mode. HRMS for measuring the exact mass was performed using a VG 70-250-S mass spectrometer (magnetic sector, EI) or Agilent 6230 TOF HPLC-MS with a jet stream ESI source.

Spectral data for UV−vis absorption were acquired in a PerkinElmer Lamda 20 spectrophotometer.

UPLC analysis was performed for homogeneity analysis and compound characterization in a Waters Acquity System combined with a photodiode array (PDA) detector. The UPLC analysis involved running a sample in a C4 BEH column (100 × 2.1 mm, 300 Å) at a flow rate of 0.2 mL min^{-1}. The elution occurred in a linear gradient composed of two mobile solvents, water and acetonitrile, each containing TFA (0.1% v/v) (eluents A and B, respectively). Its method consisted of an initial phase 1% B (0−1.4 min), a linear increase to 80% B (1.4−13.4 min), a decrease to 50% B (13.4−13.8 min), a decrease to 1% B (13.8−14.4 min), and finally an isocratic elution at 1% B (14.4−18 min). This method was also applied in the kinetic analysis of product release.

Synthesis of Coumarin Cages 5 and 7 (Scheme 1). *7-(Diethylamino)-4-(hydroxymethyl)-2H-1-benzopyran-2-one (**5**).* This compound was synthesized in two steps according to our earlier protocol.[12] These involve the oxidation of 7-(diethylamino)-4-methyl-2*H*-chromen-2-one **3** to 7-(diethylamino)-2-oxo-2*H*-chromene-4-carbaldehyde **4** with selenium dioxide[12,64] and reduction of the aldehyde functionality to a primary alcohol using sodium borohydride.[12,23] It was characterized by ^{1}H NMR and MS, each of which was consistent with the published data including its ^{1}H NMR and UV−vis spectral data as noted here. ^{1}H NMR (500 MHz, $CDCl_3$): δ 7.34−7.32 (d, J = 10 Hz, 1H), 6.60 (br, 1H), 6.55 (s, 1H), 6.27 (s, 1H), 4.84 (s, 2H), 3.43−3.39 (q, J = 7 Hz, 4H), 1.22−1.19 (t, J = 7 Hz, 6H) ppm. UV−vis spectroscopy ([**5**] = 5.05 × 10^{-5} M in 35% aq methanol): λ_{max} 387 nm (ε = 22,687 M^{-1} cm^{-1}), 249 nm (ε = 17,014 M^{-1} cm^{-1}) (see Figure 2).

*4-((7-(Diethylamino)-2-oxo-2H-1-benzopyran-4-yl)methoxy])-benzaldehyde (**6**).* First, **5** was derivatized to its methanesulfonate according to Wong et al.[12] This was used immediately without further purification. TLC analysis: R_f (2% methanol/dichloromethane) = 0.44. MS (ESI) m/z (relative intensity, %) = 326 (100%) [M + H]$^+$.

Second, potassium carbonate (464 mg, 3.36 mmol) was added to 4-hydroxybenzaldehyde (164 g, 1.34 mmol) in anhydrous THF (12 mL). The mixture was stirred at 45 °C for 10 min prior to adding a solution of 7-diethylaminocoumarin-4-hydroxylmethyl methanesulfonate **5** (365 mg, 1.12 mmol) in anhydrous THF (3 mL). The mixture was stirred continuously for 4 h, followed by filtration and concentration in vacuo. The residue was purified by flash column chromatography by eluting with a mixture of dichloromethane/ethyl acetate/hexanes (1:1:2). The product **6** was obtained as a yellow solid (235 mg, 60%). TLC analysis: R_f (1:1:2 dichloromethane/ethyl acetate/hexanes) = 0.33. MS (ESI) m/z (relative intensity, %) = 352.1 (100) [M + H]$^+$. HRMS (EI) [M + H]$^+$ m/z: calcd for $C_{21}H_{22}NO_4^+$, 352.1549; found, 352.1544. ^{1}H NMR (500 MHz, DMSO-d_6): δ 9.90 (s, 1H), 7.92−7.90 (d, J = 10 Hz, 2H), 7.60−7.58 (d, J = 10 Hz, 1H), 7.33−7.31 (d, J = 10 Hz, 2H), 6.73−6.71 (d, J = 10 Hz, 1H), 6.56 (s, 1H), 6.14 (s, 1H), 5.46 (s, 2H), 3.46−3.42 (q, J = 7 Hz, 4H), 1.11−1.14 (t, J = 7 Hz, 6H) ppm. ^{13}C{^{1}H} NMR (100

https://dx.doi.org/10.1021/acs.joc.9b02617
J. Org. Chem. XXXX, XXX, XXX−XXX

MHz, DMSO-d_6): δ 191.4, 191.3, 162.5, 160.7, 155.8, 150.8, 150.5, 131.8, 131.8, 130.2, 125.8, 125.6, 115.5, 115.3, 108.7, 105.2, 105.1, 96.9, 96.8, 65.6, 44.1, 44.0, 43.9, 12.33, 12.25 ppm.

*7-(Diethylamino)-4-[(4-(hydroxymethyl)phenoxy)methyl]-2H-1-benzopyran-2-one (**7**).* To a cold solution of **6** (200 mg, 0.626 mmol) in methanol (4 mL) in an ice bath was added sodium borohydride (23 mg, 0.626 mmol). The mixture was stirred at the same temperature for 30 min, and the reaction was quenched by adding 0.1 M sodium hydroxide solution (1 mL). The solution was concentrated in vacuo, and the residue was dissolved in dichloromethane (10 mL). After washing with water, the organic layer was dried over sodium sulfate and concentrated in vacuo, yielding a residue, which was purified by flash column chromatography by eluting with a mixture of dichloromethane/ethyl acetate/hexanes (1:1:1). The desired product 7 was obtained as a yellow solid (168 mg, 84%). TLC analysis: R_f (1:1:1 dichloromethane/ethyl acetate/hexanes) = 0.39. MS (ESI) m/z (relative intensity, %) = 354.1 (100). HRMS (ESI-TOF) $[M + H]^+$ m/z: calcd for $C_{21}H_{24}NO_4^+$, 354.1705; found, 354.1711. ^{1}H NMR (500 MHz, CD_3OD): 7.58−7.56 (d, J = 10 Hz, 1H), 7.32−7.30 (d, J = 10 Hz, 2H), 7.04−7.02 (d, J = 10 Hz, 2H), 6.77−6.75 (dd, J_1 = 5 Hz, J_2 = 10 Hz, 1H), 6.57−6.56 (d, J = 5 Hz, 1H), 6.20 (s, 1H), 5.29 (s, 2H), 4.53 (s, 2H), 3.50−3.46 (q, J = 7 Hz, 4H), 1.23−1.20 (t, J = 7 Hz, 6H) ppm. ^{13}C{^{1}H} NMR (100 MHz, DMSO-d_6): 160.7, 156.5, 155.8, 151.7, 150.4, 135.4, 128.0, 127.9, 125.7, 125.6, 114.5, 108.7, 105.4, 105.2, 105.1, 96.9, 96.8, 65.2, 62.5, 44.0, 43.9, 12.33, 12.26 ppm.

Synthesis of 1 dT$^{O\text{-}DEACM}$ (Scheme 1). Synthesis of **1** was performed according to Rodrigues-Correia et al.[23] Its characterization data are consistent with those values reported therein or as anticipated, confirming its structural identity.

*1-((2R,4S,5R)-4-(tert-Butyldimethylsilyl)oxy-5-(((tert-butyldimethylsilyl)oxy)methyl)tetrahydrofuran-2-yl)-5-methylpyrimidine-2,4(1H,3H)-dione (**9**).* Protection of thymidine through O-TBDMS was performed according to an established protocol in the literature.[23,43] To a solution of thymidine (0.60 g, 2.48 mmol) in dimethylformamide (DMF; 2.2 mL) were added *tert*-butyldimethylsilyl chloride (TBDMS-Cl) (1.49 g, 9.91 mmol) and imidazole (1.18 g, 17.34 mmol). The mixture was stirred at room temperature overnight, and its reaction was quenched by adding ethanol (2 mL), followed by stirring for 30 min. It was diluted with ethyl acetate (50 mL), and the white solid, which was precipitated, was filtered off and washed with ethyl acetate (10 mL). The organic solutions were combined, washed with water (3 × 50 mL) and brine (50 mL), and then dried over sodium sulfate. Concentration of the solution in vacuo afforded the product **9** as a white solid (1.19 g, 100%). TLC analysis: R_f (1:10 methanol/dichloromethane) = 0.45. MS (ESI) m/z (relative intensity, %) = 493.2 (100) $[M + Na]^+$, 963.5 (50) $[2M + Na]^+$. HRMS (ESI-TOF) m/z: $[M + Na]^+$ calcd for $C_{22}H_{42}N_2NaO_5Si_2^+$, 493.2530; found, 493.2523. ^{1}H NMR (500 MHz, CD_3OD): 7.54 (s, 1H), 6.25−6.23 (t, J = 5 Hz, 1H), 4.48−4.46 (m, 1H), 3.93−3.91 (m, 1H), 3.87−3.79 (m, 2H), 2.23−2.10 (m, 2H), 1.87 (s, 3H), 0.93−0.91 (s, 18H), 0.12−0.11 (s, 12H) ppm.

*1-((2R,4S,5R)-4-((tert-Butyldimethylsilyl)oxy)-5-(((tert-butyldimethylsilyl)oxy)methyl)tetrahydrofuran-2-yl)-5-methyl-4-(1H-1,2,4-triazol-1-yl)pyrimidin-2(1H)-one (**10**).* Substitution of *O*-TBDMS protected thymidine with 1,2,4-1*H*-triazole at the C_4 position was performed according to a protocol reported in the literature.[23,43] To a cold solution of 1,2,4-1*H*-triazole (10.4 g, 150.8 mmol) in anhydrous acetonitrile (43.5 mL) in an ice bath were added phosphoryl chloride (3.1 mL, 33.28 mmol) and then triethylamine (22.9 mL, 164.2 mmol), each in a dropwise manner. After stirring for 15 min, a solution of **9** (1.0 g, 2.12 mmol) in anhydrous acetonitrile (16.9 mL) was added to the mixture. The final mixture was heated to room temperature and stirred overnight. To quench the reaction, a saturated solution of sodium bicarbonate (10 mL) was added to the mixture, and it was stirred for 30 min. Volatile solvents were removed by concentration in vacuo, and the residue was extracted with dichloromethane (45 mL). The organic solution was washed with saturated sodium bicarbonate (30 mL), water (30 mL), and brine (30 mL), dried over sodium sulfate, and evaporated in vacuo. The residue was purified by column chromatography by eluting with ethyl acetate/hexanes/dichloromethane (1:1:1), yielding **10** as a white solid (0.94 g, 85%). TLC analysis: R_f (ethyl acetate/hexanes/dichloromethane; 1:1:1) = 0.17. MS (ESI) m/z (relative intensity, %) = 522.2 (20) $[M + H]^+$, 544.2 (17) $[M + Na]^+$, 1043.5 (75) $[2M + H]^+$, 1065.5 (100) $[2M + Na]^+$. HRMS (ESI-TOF) m/z: $[M + H]^+$ calcd for $C_{24}H_{44}N_5O_4Si_2^+$, 522.2932; found, 522.2927; $[M + Na]^+$ calcd for $C_{24}H_{43}N_5NaO_4Si_2^+$, 544.2751; found, 544.2745. ^{1}H NMR (500 MHz, CD_3OD): 9.33 (s, 1H), 8.38 (s, 1H), 8.24 (s, 1H), 6.22−6.20 (t, J = 5 Hz, 1H), 4.49−4.47 (m, 1H), 4.13−4.11 (m, 1H), 3.98−3.85 (m, 2H), 2.63−2.58 (m, 1H), 2.45 (s, 3H), 2.21−2.16 (m, 1H), 0.93−0.91 (s, 18H), 0.14−0.13 (s, 12H) ppm. ^{13}C{^{1}H} NMR (100 MHz, DMSO-d_6): 157.9, 153.41, 153.35, 152.9, 147.1, 145.3, 145.2, 104.4, 88.1, 87.9, 87.2, 87.1, 71.9, 71.8, 62.4, 40.9, 25.72, 25.65, 25.6, 17.9, 17.7, 16.2, 16.1, −4.77, −4.82, −4.97, −5.02, −5.6 ppm.

*4-((7-(Diethylamino)-2-oxo-2H-1-benzopyran-4-yl)methoxy)-1-((2R,4S,5R)-4-((tert-butyldimethylsilyl)oxy)-5-(((tert-butyldimethylsilyl)oxy)methyl)tetrahydrofuran-2-yl)-5-methylpyrimidin-2(1H)-one (**11**).* To a solution of **5** (420 mg, 1.70 mmol) and **10** (970 mg, 1.86 mmol) dissolved in anhydrous acetonitrile (14 mL) was added 1,8-diazabicyclo[5,4,0]undec-7-ene (0.28 mL, 1.86 mmol). The mixture was stirred at room temperature overnight and then concentrated in vacuo. The residue was purified by column chromatography by eluting with ethyl acetate/hexanes/dichloromethane (1:2:1), yielding **11** as a pale yellow foam (1.11 g, 97%). TLC analysis: R_f (ethyl acetate/hexanes/dichloromethane; 1:2:1) = 0.62. MS (ESI) m/z (relative intensity, %) = 700.38 (55) $[M + H]^+$, 1400.75 (45) $[2M + H]^+$. HRMS (ESI-TOF) m/z: $[M + H]^+$ calcd for $C_{36}H_{58}N_3O_7Si_2^+$, 700.3813; found, 700.3806. ^{1}H NMR (500 MHz, DMSO-d_6: 7.82 (s, 1H), 7.51−7.49 (d, J = 10 Hz, 1H), 6.72−6.70 (d, J = 10 Hz, 1H), 6.55 (s, 1H), 6.15−6.12 (t, J = 5 Hz, 1H), 5.97 (s, 1H), 5.59−5.52 (m, 2H), 4.36 (s, 1H), 3.89 (s, 1H), 3.88−3.72 (m, 2H), 3.45−3.41 (q, J = 7 Hz, 4H), 2.24−2.22 (m, 1H), 2.15−2.10 (m, 1H), 1.98 (s, 3H), 1.13−1.10 (t, J = 7 Hz, 6H), 0.87 (s, 18H), 0.08 (s, 12H) ppm. ^{13}C{^{1}H} NMR (500 MHz, DMSO-d_6): 168.8, 160.6, 155.8, 154.2, 150.53, 150.47, 141.1, 125.4, 108.8, 105.2, 104.9, 102.9, 96.8, 87.3, 85.7, 72.0, 63.4, 62.6, 44.0, 40.5, 26.3, 25.7, 25.6, 17.9, 17.7, 12.3, 11.8, −4.8, −5.0, −5.5 ppm.

*4-((7-(Diethylamino)-2-oxo-2H-1-benzopyran-4-yl)methoxy)-1-((2R,4S,5R)-4-hydroxy-5-(hydroxymethyl)tetrahydrofuran-2-yl)-5-methylpyrimidin-2(1H)-one (**1**).* To a solution of **11** (1.09 g, 1.56 mmol) in THF (3.6 mL) was added acetic acid (0.88 mL). The mixture was stirred at room temperature for 10 min, followed by the addition of 1 M TBAF in THF (4.7 mL). The mixture was stirred overnight and evaporated in vacuo. The residue was triturated and washed with saturated sodium bicarbonate solution (3 × 10 mL), water (5 × 10 mL), and ethyl acetate/hexane (1:1; 3 × 10 mL). The desired product **1** was obtained as an orange white solid (0.6 g, 82%). TLC analysis: R_f (cyclohexane/acetone; 1:1) = 0.1. UPLC: t_r = 8.72 min (homogeneity ≥ 95%). MS (ESI) m/z (relative intensity, %) = 494.1 (30) $[M + Na]^+$, 943.4 (16) $[2M + H]^+$, 965.3 (30) $[2M + Na]^+$. HRMS (ESI-TOF) m/z: $[M + Na]^+$ calcd for $C_{24}H_{29}N_3NaO_7^+$, 494.1903; found, 494.1898. ^{1}H NMR (500 MHz, DMSO-d_6): 8.13 (s, 1H), 7.51−7.49 (d, J = 10 Hz, 1H), 6.73−6.71 (dd, J_1 = 3 Hz, J_2 = 10 Hz, 1H), 6.56−6.55 (d, J = 3 Hz, 1H), 6.15−6.12 (t, J = 5 Hz, 1H), 5.98 (s, 1H), 5.56 (s, 2H), 4.24 (m, 1H), 3.83−3.81 (m, 1H), 3.66−3.56 (m, 2H), 3.46−3.42 (q, J = 7 Hz, 2H), 2.24−2.19 (m, 1H), 2.06−2.00 (m, 1H), 1.98 (s, 3H), 1.14−1.11 (t, J = 7 Hz, 6H) ppm. ^{13}C{^{1}H} NMR (100 MHz, DMSO-d_6): 168.7, 160.6, 155.8, 154.3, 150.6, 150.5, 141.8, 125.5, 125.4, 108.81, 108.78, 105.2, 104.9, 104.7, 102.8, 96.9, 96.8, 87.7, 87.6, 85.7, 85.5, 69.93, 69.85, 63.3, 60.9, 44.1, 44.0, 43.9, 40.6, 12.32, 12.25, 11.82, 11.78 ppm. UV−vis spectroscopy ([**1**] = 1.06 × 10^{-4} M in 35% aq methanol): λ_{max} = 393 nm (ε = 10,209 M^{-1} cm^{-1}), 282 nm (ε = 5926 M^{-1} cm^{-1}), 254 nm (ε = 8721 M^{-1} cm^{-1}) (see Figure 2).

Synthesis of 2 dT$^{O\text{-}Bn\text{-}DEACM}$ (Scheme 1). *4-((4-((7-(Diethylamino)-2-oxo-2H-1-benzopyran-4-yl)methoxy)benzyl)oxy)-1-((2R,4S,5R)-4-((tert-butyldimethylsilyl)oxy)-5-(((tert-butyldimethylsilyl)oxy)methyl)tetrahydrofuran-2-yl)-5-methylpyrimidin-2(1H)-one (**12**).* To a solution of **7** (290 mg, 0.82 mmol) and **10** (471 mg, 0.90 mmol) dissolved in acetonitrile (6 mL) was added

https://dx.doi.org/10.1021/acs.joc.9b02617
J. Org. Chem. XXXX, XXX, XXX−XXX

1,8-diazabicyclo[5,4,0]undec-7-ene (0.135 mL, 0.90 mmol). The mixture was stirred at room temperature overnight and then concentrated in vacuo. The residue was purified by column chromatography by eluting with ethyl acetate/hexanes/dichloromethane (1:3:1), yielding **12** as a pale yellow foam (615 mg, 93%). TLC analysis: R_f (ethyl acetate/hexanes/dichloromethane; 1:2:1) = 0.40. HRMS (ESI-TOF) m/z: $[M + H]^+$ calcd for $C_{43}H_{64}N_3O_8Si_2^+$, 806.4232; found, 806.4223. ^{1}H NMR (500 MHz, DMSO-d_6): δ 7.74 (s, 1H), 7.59−7.57 (d, J = 10 Hz, 1H), 7.43−7.41 (d, J = 10 Hz, 2H), 7.13−7.11 (d, J = 10 Hz, 2H), 6.72−6.70 (d, J = 10 Hz, 1H), 6.55 (s, 1H), 6.16−6.14 (t, J = 5 Hz, 1H), 6.12 (s, 1H), 5.33 (s, 2H), 5.28 (s, 2H), 4.36 (s, 1H), 3.86 (s, 1H), 3.80−3.72 (m, 2H), 3.45−3.41 (q, J = 7 Hz, 4H), 2.22−2.20 (m, 1H), 2.13−2.07 (m, 1H), 1.88 (s, 3H), 1.13−1.10 (t, J = 7 Hz, 6H), 0.87−0.86 (s, 18H), 0.08−0.07 (s, 12H) ppm. ^{13}C{^{1}H} NMR (100 MHz, DMSO-d_6): 169.4, 160.7, 157.6, 155.8, 154.4, 151.4, 150.4, 140.4, 129.9, 128.8, 125.7, 114.8, 108.7, 105.4, 105.2, 103.1, 96.8, 87.2, 85.5, 72.0, 67.6, 65.3, 62.6, 44.0, 40.4, 25.7, 25.6, 17.9, 17.7, 12.3, 11.9, −4.8, −5.0, −5.5 ppm.

*4-((4-((7-(Diethylamino)-2-oxo-2H-1-benzopyran-4-yl)methoxy)-benzyl)oxy)-1-((2R,4S,5R)-4-hydroxy-5-(hydroxymethyl)-tetrahydrofuran-2-yl)-5-methylpyrimidin-2(1H)-one (**2** dT$^{O\text{-}Bn\text{-}DEACM}$).* Acetic acid (0.46 mL) was added to a solution of **12** (530 mg, 0.66 mmol) in THF (2.3 mL). The mixture was stirred at room temperature for 10 min, followed by the addition of 1 M TBAF in THF (2 mL). The mixture was stirred overnight, and the mixture was diluted with diethyl ether (20 mL), which led to precipitation of the product as a pale yellow solid. It was collected, triturated, and washed with saturated sodium bicarbonate (3 × 10 mL), water (5 × 10 mL), ethyl acetate/hexane (1:1; 5 × 10 mL), and cyclohexane/dichloromethane/acetone (5:1:1; 10 mL). The solid was dried in vacuo, yielding **2** as a pale yellow solid (270 mg, 71%). A TLC analysis showed only one spot with an R_f (cyclohexane/acetone; 1:2) value of 0.3. UPLC: t_r = 9.32 min (homogeneity ≥ 95%). MS (ESI) m/z (relative intensity, %) = 230.1 and 336.1 (100), 578.2 (30) $[M + H]^+$, 600.2 (15) $[M + Na]^+$. HRMS (ESI-TOF) m/z: $[M + H]^+$ calcd for $C_{21}H_{35}N_3O_8^+$, 578.2502; found, 578.2496. ^{1}H NMR (500 MHz, CD_3OD): 8.15 (s, 1H), 7.58−7.56 (d, J = 10 Hz, 1H), 7.46−7.44 (d, J = 10 Hz, 2H), 7.06−7.08 (d, J = 10 Hz, 2H), 6.76−6.74 (dd, J_1 = 3 Hz, J_2 = 10 Hz, 1H), 6.57−6.56 (d, J = 3 Hz, 1H), 6.26−6.24 (t, J = 5 Hz, 1H), 6.21 (s, 1H), 5.37 (s, 2H), 5.30 (s, 2H), 4.38−4.36 (m, 1H), 3.95−3.94 (m, 1H), 3.84−3.72 (m, 2H), 3.50−3.46 (q, J = 7 Hz, 4H), 2.41−2.38 (m, 1H), 2.17−2.13 (m, 1H), 1.96 (s, 3H), 1.23−1.20 (t, J = 7 Hz, 6H) ppm. ^{13}C{^{1}H} NMR (100 MHz, DMSO-d_6): 169.3, 160.7, 157.6, 155.8, 154.5, 151.5, 150.4, 141.11, 141.05, 130.0, 129.8, 128.9, 125.8, 125.6, 114.9, 114.7, 108.7, 105.6, 105.3, 105.1, 102.9, 96.9, 96.8, 87.6, 87.5, 85.5, 85.3, 70.0, 69.9, 67.4, 65.3, 61.0, 44.0, 43.9, 40.6, 12.34, 12.25, 11.9 ppm. UV−vis spectroscopy ([**2**] = 8.67 × 10^{-5} M in 35% aq methanol): λ_{max} = 390 nm (ε = 11,603 M^{-1} cm^{-1}), 277 nm (ε = 8133 M^{-1} cm^{-1}), 252 nm (ε = 11,773 M^{-1} cm^{-1}) (see Figure 2).

Synthesis of dT$^{N\text{-}DEACM}$ (Scheme S1). *3-((7-(Diethylamino)-2-oxo-2H-1-benzopyran-4-yl)methyl)-1-((2R,4S,5R)-4-hydroxy-5-(hydroxymethyl)tetrahydrofuran-2-yl)-5-methylpyrimidine-2,4-(1H,3H)-dione (dT$^{N\text{-}DEACM}$).* Synthesis of **dT**$^{N\text{-}DEACM}$ was performed by N-alkylation of thymidine (**dT**) at the 3 position with 7-diethylaminocoumarinyl-4-methyl bromide[74] according to the condition reported by Yoshida et al.[44]

To a cold solution of **5** (160 mg, 0.65 mmol) and triethylamine (272 μL, 1.95 mmol) in dichloromethane (4 mL) in an ice water bath was added methanesulfonyl chloride (182 μL, 2.34 mmol). This reaction mixture was stirred in an ice bath for 1 h prior to dilution with dichloromethane (4 mL). The solution was washed several times using 0.5 N HCl (2 × 5 mL), saturated $NaHCO_3$ solution (5 mL), water (5 mL), and brine (5 mL). The organic layer was dried over anhydrous Na_2SO_4 and concentrated in vacuo, yielding 7-diethylaminocoumarinyl-4-methyl methanesulfonate, which was used immediately.

To this derivative dissolved in THF (5 mL) was added lithium bromide (113 mg, 1.3 mmol). This mixture was stirred at room temperature for 3 h to produce 7-diethylaminocoumarinyl-4-methyl bromide.[74] This reaction mixture was diluted with acetone (5 mL), followed by the addition of thymidine (236 mg, 0.98 mmol) and potassium carbonate (270 mg, 1.95 mmol). The mixture was stirred at 55 °C for 48 h and concentrated in vacuo. The residue was purified by silica column chromatography by eluting with a mixture of acetone and cyclohexanes (1:1), affording a brown solid. It was rinsed with dichloromethane (3 × 1 mL) and then dried under high vacuum, yielding **dT**$^{N\text{-}DEACM}$ as a pale yellow solid (140 mg, 37%). TLC analysis: R_f (1:1 acetone/cyclohexanes) = 0.36. UPLC traces acquired for **dT**$^{N\text{-}DEACM}$ show that it elutes at t_r = 8.57 min slightly faster than **1** at t_r = 8.72 min (Figure S12). Its structural identity was confirmed through spectroscopic characterization. MS (ESI) m/z (relative intensity, %) = 472.20 (100) $[M + H]^+$, 494.19 (10) $[M + Na]^+$. HRMS (ESI-TOF) m/z: $[M + H]^+$ calcd for $C_{24}H_{30}N_3O_7^+$, 472.2084; found, 472.2079. ^{1}H NMR (500 MHz, DMSO-d_6): 7.91 (s, 1H), 7.68−7.66 (d, J = 10 Hz, 1H), 6.75−6.72 (dd, J_1 = 5 Hz, J_2 = 10 Hz, 1H), 6.56−6.55 (d, J = 5 Hz, 1H), 6.22−6.19 (t, J = 7.5 Hz, 1H), 5.43 (s, 1H), 5.25−5.24 (d, J = 5 Hz, 1H), 5.12 (s, 2H), 5.08−5.06 (t, J = 5 Hz, 1H), 4.27−4.26 (m, 1H), 3.80−3.78 (m, 1H), 3.63−3.58 (m, 2H), 3.46−3.43 (q, J = 5Hz, 4H), 2.20−2.13 (m, 2H), 1.88 (s, 3H), 1.14−1.12 (t, J = 5 Hz, 6H) ppm. ^{13}C{^{1}H} NMR (100 MHz, DMSO-d_6): 162.5, 160.6, 155.7, 151.1, 150.5, 150.3, 135.6, 125.3, 108.8, 108.4, 105.8, 103.0, 96.8, 87.4, 85.1, 70.1, 61.1, 44.0, 40.6, 39.6, 12.9, 12.3 ppm.

Synthesis of 2 dT$^{O\text{-}Bn\text{-}DEACM}$ Phosphoramidite (Scheme 2). *1-((2R,4S,5R)-5-((Bis(4-methoxyphenyl)(phenyl)methoxy)methyl)-4-hydroxytetrahydrofuran-2-yl)-4-((4-((7-(diethylamino)-2-oxo-2H-1-benzopyran-4-yl)methoxy)benzyl)oxy)-5-methylpyrimidin-2(1H)-one (**13**).* O-Protection with a 4,4′-dimethoxytrityl (DMT) group was performed by adding 4,4′-dimethoxytrityl chloride (182 mg, 0.54 mmol) to **2** (248 mg, 0.43 mmol) in pyridine (6.5 mL) cooled at 0 °C. The mixture was stirred overnight while allowing it to warm up to room temperature. The reaction was quenched by adding ethanol (0.2 mL), and the reaction mixture was evaporated in vacuo and then coevaporated with toluene (3 × 10 mL) to remove any residual pyridine. The crude product was purified by column chromatography by eluting with cyclohexane/acetone (1:1), yielding **13** as a pale yellow solid (230 mg, 61%). TLC analysis: R_f (cyclohexane/acetone; 1:2) = 0.50. UPLC: t_r = 12.15 min (homogeneity ≥ 95%). MS (ESI) m/z (relative intensity, %) = 902.3 (90) $[M + Na]^+$. HRMS (ESI-TOF) m/z: $[M + Na]^+$ calcd for $C_{52}H_{53}N_3NaO_{10}^+$, 902.3629; found, 902.3618. ^{1}H NMR (500 MHz, CD_3OD): 8.02 (s, 1H), 7.57−7.55 (d, J = 10 Hz, 1H), 7.45−7.43 (d, J = 10 Hz, 2H), 7.40−7.39 (d, J = 5 Hz, 2H), 7.30−7.25 (m, 6H), 7.22−7.19 (m, 1H), 7.08−7.06 (d, J = 10 Hz, 2H), 6.85−6.84 (d, J = 5 Hz, 4H), 6.76−6.74 (dd, J_1 = 3 Hz, J_2 = 10 Hz, 1H), 6.56−6.55 (d, J = 3 Hz, 1H), 6.28−6.25 (t, J = 5 Hz, 1H), 6.21 (s, 1H), 5.40−5.33 (m, 2H), 5.30 (s, 2H), 4.51−4.50 (m, 1H), 4.06−4.05 (m, 1H), 3.76 (s, 6H), 3.50−3.47 (m, 4H), 3.45−3.34 (m, 2H), 2.51−2.48 (m, 1H), 2.33−2.29 (m, 1H), 1.50 (s, 3H), 1.22−1.19 (t, J = 7 Hz, 6H) ppm. ^{13}C{^{1}H} NMR (100 MHz, DMSO-d_6): 169.4, 160.7, 158.1, 157.6, 155.8, 151.4, 150.4, 144.7, 140.5, 135.4, 135.2, 129.9, 129.7, 128.8, 127.9, 127.6, 126.8, 125.7, 114.8, 113.2, 108.7, 105.4, 105.2, 103.2, 96.8, 85.9, 85.7, 85.4, 70.1, 67.5, 65.3, 63.4, 55.0, 44.0, 40.7, 12.3, 11.4 ppm.

*1-((2R,4S,5R)-5-((Bis(4-methoxyphenyl)(phenyl)methoxy)-methyl)-4-(((2-cyanoethyl)-N,N-bis(1-methylethyl)phosphino)oxy)-tetrahydrofuran-2-yl)-4-((4-((7-(diethylamino)-2-oxo-2H-1-benzo-pyran-4-yl)methoxy)benzyl)oxy)-5-methylpyrimidin-2(1H)-one (**14**).* To a solution of **13** (140 mg, 0.16 mmol) dissolved in anhydrous dichloromethane (5 mL) were added in sequence DIPEA (0.14 mL, 0.8 mmol) and then 2-cyanoethyl *N*,*N*-diisopropylchlorophosphoramidite (71 μL, 0.32 mmol). The mixture was stirred for 2 h, diluted with dichloromethane (5 mL), and washed extensively with saturated sodium bicarbonate (2 × 5 mL), water (5 mL), and brine (5 mL). The organic layer was evaporated in vacuo, and the residue was purified by column chromatography by eluting with cyclohexane/dichloromethane/acetone (2:1:1). The desired product **14** was obtained as a yellow solid (126 mg, 73%). UPLC is not applicable for its analysis because of the aqueous instability of its phosphoramidite moiety. TLC analysis: a single spot with R_f (cyclohexane/dichloromethane/acetone; 2:1:1) of 0.39. MS (ESI)

https://dx.doi.org/10.1021/acs.joc.9b02617
J. Org. Chem. XXXX, XXX, XXX−XXX

m/z (relative intensity, %) = 1080.4 (20) $[M + H]^+$, 1102.4 (30) $[M + Na]^+$. HRMS (ESI-TOF) m/z: $[M + Na]^+$ calcd for $C_{61}H_{70}N_5NaO_{11}P^+$, 1102.4707; found, 1102.4696. ^1H NMR (500 MHz, CD_3OD): 7.85 (s, 1H), 7.59−7.57 (d, J = 10 Hz, 1H), 7.43−7.41 (d, J = 10 Hz, 2H), 7.38−7.37 (d, J = 5 Hz, 2H), 7.30−7.21 (m, 7H), 7.13−7.11 (d, J = 10 Hz, 2H), 6.88−6.86 (dd, J_1 = 3 Hz, J_2 = 10 Hz, 4H), 6.73−6.71 (dd, J_1 = 3 Hz, J_2 = 10 Hz, 1H), 6.56−6.55 (d, J = 3 Hz, 1H), 6.22−6.20 (t, J = 10 Hz, 1H), 6.13 (s, 1H), 5.34 (s, 2H), 5.29 (s, 2H), 4.54−4.53 (m, 1H), 4.05−4.06 (m, 1H), 3.72 (s, 6H), 3.74−3.68 (m, 2H), 3.52−3.47 (m, 2H), 3.46−3.42 (q, J = 10 Hz, 4H), 2.77−2.75 (t, J = 10 Hz, 2H), 2.48−2.43 (m), 2.33−2.29 (m, 1H), 1.57 (s, 3H), 1.13−1.10 (m, 12H), 0.98−0.97 (d, J = 5 Hz, 6H) ppm. $^{13}C\{^1H\}$ NMR (100 MHz, DMSO-d_6): 169.4, 160.7, 158.2, 157.6, 155.8, 154.3, 151.4, 150.4, 144.5, 140.6, 135.2, 135.1, 129.9, 129.7, 128.8, 127.9, 127.6, 126.8, 125.7, 118.9, 114.8, 113.2, 108.7, 105.4, 105.2, 103.4, 96.8, 86.0, 85.4, 84.4, 67.6, 65.3, 62.8, 58.3, 58.2, 55.0, 46.2, 44.0, 42.6, 42.5, 29.6, 26.3, 24.3, 24.2, 24.1, 22.2, 20.7, 19.8, 19.2, 18.8, 12.3, 11.4 ppm.

Photon Uncaging Experiments. *Light Sources.* Photolytic studies for thymidine release were performed with three light sources (Luzchem Research). These include (i) a UVA lamp with a maximal intensity at 365 nm; (ii) a visible light lamp at 420 nm (LZC-420); and (iii) a light-emitting diode lamp for blue light 445−465 nm (LZC-LBL). Photon flux density ($q_{n,p} = q_p/N_A$, mol × s^{-1}) of each lamp was determined by ferrioxalate actinometry according to a standard protocol.[67,68] Photon flux density ($q_{n,p} = q_p/N_A$, mol × s^{-1}) determined for each lamp by ferrioxalate actinometry is summarized in Table S2 (Supporting Information).

Uncaging Kinetics and Analysis. Typically, a solution of caged thymidine **1** or **2** ($\mathbf{dT}^{caged}$: 0.05−0.1 mg/mL) in aq methanol (30−35% v/v) was prepared and exposed to the light at a distance of ∼5 cm. After each exposure period, the solution was aliquoted out as a function of irradiation time (0−30 min), and each aliquot was analyzed by UPLC and UV−vis absorption spectrometry to determine the kinetics of thymidine release and byproduct formation. Certain aliquots were further analyzed by HPLC-MS (ESI) to validate the identity of thymidine and released molecular species in the photolyzed solution.

Quantum efficiency (Φ) for the release of thymidine ($\mathbf{dT}$) is defined in eq 1, and its value was calculated according to a standard method as noted in eq 2[68]

$$\Phi_{release} = [\text{number of thymidine released}] / [\text{number of photon absorbed}] \quad (1)$$

$$\Phi_{release} = (\Delta \mathbf{dT}/\Delta t)/(q_{n,p}(1 - 10^{-A})) \quad (2)$$

where $q_{n,p}$ refers to the photon flux density (mol × s^{-1}), $\Delta\mathbf{dT}/\Delta t$ refers to the rate of thymidine release (mol × s^{-1}), and A refers to the absorbance of caged thymidine at the specific wavelength of light irradiated.

■ ASSOCIATED CONTENT

Supporting Information

The Supporting Information is available free of charge at https://pubs.acs.org/doi/10.1021/acs.joc.9b02617.

Summary of photo physicochemical properties 1 and 2; summary of photon flux density; synthetic scheme of $\mathbf{dT}^{N\text{-DEACM}}$; copies of spectral data; UPLC traces for photouncaging; and HPLC-MS analysis of photolysis products from 1 (PDF)

■ AUTHOR INFORMATION

Corresponding Author

Seok Ki Choi − *Michigan Nanotechnology Institute for Medicine and Biological Sciences and Department of Internal Medicine, University of Michigan Medical School, Ann Arbor, Michigan 48109, United States;* orcid.org/0000-0001-5633-4817; Email: skchoi@umich.edu

Authors

Shengzhuang Tang − *Michigan Nanotechnology Institute for Medicine and Biological Sciences and Department of Internal Medicine, University of Michigan Medical School, Ann Arbor, Michigan 48109, United States*

Jayme Cannon − *Michigan Nanotechnology Institute for Medicine and Biological Sciences and Department of Internal Medicine, University of Michigan Medical School, Ann Arbor, Michigan 48109, United States*

Kelly Yang − *Michigan Nanotechnology Institute for Medicine and Biological Sciences, University of Michigan Medical School, Ann Arbor, Michigan 48109, United States*

Matthew F. Krummel − *Department of Pathology, University of California, San Francisco, San Francisco, California 94143, United States*

James R. Baker, Jr. − *Michigan Nanotechnology Institute for Medicine and Biological Sciences and Department of Internal Medicine, University of Michigan Medical School, Ann Arbor, Michigan 48109, United States;* orcid.org/0000-0002-4478-1932

Complete contact information is available at: https://pubs.acs.org/10.1021/acs.joc.9b02617

Notes

The authors declare no competing financial interest.

■ ACKNOWLEDGMENTS

This work was supported in part by the National Cancer Institute, National Institutes of Health under award 1R21CA191428. S.K.C. acknowledges support from the Michigan Nanotechnology Institute for Medicine and Biological Sciences, University of Michigan Medical School.

■ ABBREVIATIONS

dT, thymidine; DEACM, 7-diethylamino-4-methylcoumarin; UPLC, ultraperformance liquid chromatography

■ REFERENCES

(1) Klán, P.; Šolomek, T.; Bochet, C. G.; Blanc, A.; Givens, R.; Rubina, M.; Popik, V.; Kostikov, A.; Wirz, J. Photoremovable Protecting Groups in Chemistry and Biology: Reaction Mechanisms and Efficacy. *Chem. Rev.* **2013**, *113*, 119−191.

(2) Kaplan, J. H.; Forbush, B.; Hoffman, J. F. Rapid photolytic release of adenosine 5′-triphosphate from a protected analog: utilization by the sodium:potassium pump of human red blood cell ghosts. *Biochemistry* **1978**, *17*, 1929−1935.

(3) Billington, A. P.; Walstrom, K. M.; Ramesh, D.; Guzikowski, A. P.; Carpenter, B. K.; Hess, G. P. Synthesis and photochemistry of photolabile N-glycine derivatives and effects of one on the glycine receptor. *Biochemistry* **1992**, *31*, 5500−5507.

(4) Brieke, C.; Rohrbach, F.; Gottschalk, A.; Mayer, G.; Heckel, A. Light-Controlled Tools. *Angew. Chem., Int. Ed.* **2012**, *51*, 8446−8476.

(5) Lee, H.-M.; Larson, D. R.; Lawrence, D. S. Illuminating the Chemistry of Life: Design, Synthesis, and Applications of "Caged" and Related Photoresponsive Compounds. *ACS Chem. Biol.* **2009**, *4*, 409−427.

(6) Amatrudo, J. M.; Olson, J. P.; Lur, G.; Chiu, C. Q.; Higley, M. J.; Ellis-Davies, G. C. R. Wavelength-Selective One- and Two-Photon Uncaging of GABA. *ACS Chem. Neurosci.* **2014**, *5*, 64−70.

(7) Kantevari, S.; Matsuzaki, M.; Kanemoto, Y.; Kasai, H.; Ellis-Davies, G. C. R. Two-color, two-photon uncaging of glutamate and GABA. *Nat. Methods* **2009**, *7*, 123.

(8) Karginov, A. V.; Zou, Y.; Shirvanyants, D.; Kota, P.; Dokholyan, N. V.; Young, D. D.; Hahn, K. M.; Deiters, A. Light Regulation of Protein Dimerization and Kinase Activity in Living Cells Using Photocaged Rapamycin and Engineered FKBP. *J. Am. Chem. Soc.* **2011**, *133*, 420−423.
(9) Lemke, E. A.; Summerer, D.; Geierstanger, B. H.; Brittain, S. M.; Schultz, P. G. Control of protein phosphorylation with a genetically encoded photocaged amino acid. *Nat. Chem. Biol.* **2007**, *3*, 769−772.
(10) Furuta, T.; Wang, S. S. H.; Dantzker, J. L.; Dore, T. M.; Bybee, W. J.; Callaway, E. M.; Denk, W.; Tsien, R. Y. Brominated 7-hydroxycoumarin-4-ylmethyls: Photolabile protecting groups with biologically useful cross-sections for two photon photolysis. *Proc. Natl. Acad. Sci. U.S.A.* **1999**, *96*, 1193−1200.
(11) Yang, Y.; Shao, Q.; Deng, R.; Wang, C.; Teng, X.; Cheng, K.; Cheng, Z.; Huang, L.; Liu, Z.; Liu, X.; Xing, B. In Vitro and In Vivo Uncaging and Bioluminescence Imaging by Using Photocaged Upconversion Nanoparticles. *Angew. Chem., Int. Ed.* **2012**, *51*, 3125−3129.
(12) Wong, P. T.; Roberts, E. W.; Tang, S.; Mukherjee, J.; Cannon, J.; Nip, A. J.; Corbin, K.; Krummel, M. F.; Choi, S. K. Control of an Unusual Photo-Claisen Rearrangement in Coumarin Caged Tamoxifen through an Extended Spacer. *ACS Chem. Biol.* **2017**, *12*, 1001−1010.
(13) Faal, T.; Wong, P. T.; Tang, S.; Coulter, A.; Chen, Y.; Tu, C. H.; Baker, J. R.; Choi, S. K.; Inlay, M. A. 4-Hydroxytamoxifen probes for light-dependent spatiotemporal control of Cre-ER mediated reporter gene expression. *Mol. BioSyst.* **2015**, *11*, 783−790.
(14) Lu, X.; Agasti, S. S.; Vinegoni, C.; Waterman, P.; DePinho, R. A.; Weissleder, R. Optochemogenetics (OCG) Allows More Precise Control of Genetic Engineering in Mice with CreER regulators. *Bioconjugate Chem.* **2012**, *23*, 1945−1951.
(15) Link, K. H.; Shi, Y.; Koh, J. T. Light Activated Recombination. *J. Am. Chem. Soc.* **2005**, *127*, 13088−13089.
(16) Lerch, M. M.; Hansen, M. J.; van Dam, G. M.; Szymanski, W.; Feringa, B. L. Emerging Targets in Photopharmacology. *Angew. Chem., Int. Ed.* **2016**, *55*, 10978−10999.
(17) Velema, W. A.; van der Berg, J. P.; Szymanski, W.; Driessen, A. J. M.; Feringa, B. L. Orthogonal Control of Antibacterial Activity with Light. *ACS Chem. Biol.* **2014**, *9*, 1969−1974.
(18) Agasti, S. S.; Laughney, A. M.; Kohler, R. H.; Weissleder, R. A photoactivatable drug-caged fluorophore conjugate allows direct quantification of intracellular drug transport. *Chem. Commun.* **2013**, *49*, 11050−11052.
(19) Wong, P. T.; Tang, S.; Mukherjee, J.; Tang, K.; Gam, K.; Isham, D.; Murat, C.; Sun, R.; Baker, J. R.; Choi, S. K. Light-Controlled Active Release of Photocaged Ciprofloxacin for Lipopolysaccharide-Targeted Drug Delivery using Dendrimer Conjugates. *Chem. Commun.* **2016**, *52*, 10357−10360.
(20) Dupart, P. S.; Mitra, K.; Lyons, C. E.; Hartman, M. C. T. Photo-controlled delivery of a potent analogue of doxorubicin. *Chem. Commun.* **2019**, *55*, 5607−5610.
(21) Lusic, H.; Young, D. D.; Lively, M. O.; Deiters, A. Photochemical DNA Activation. *Org. Lett.* **2007**, *9*, 1903−1906.
(22) Menge, C.; Heckel, A. Coumarin-Caged dG for Improved Wavelength-Selective Uncaging of DNA. *Org. Lett.* **2011**, *13*, 4620−4623.
(23) Rodrigues-Correia, A.; Knapp-Bühle, D.; Engels, J. W.; Heckel, A. Selective Uncaging of DNA through Reaction Rate Selectivity. *Org. Lett.* **2014**, *16*, 5128−5131.
(24) Rodrigues-Correia, A.; Weyel, X. M. M.; Heckel, A. Four Levels of Wavelength-Selective Uncaging for Oligonucleotides. *Org. Lett.* **2013**, *15*, 5500−5503.
(25) Ceo, L. M.; Koh, J. T. Photocaged DNA Provides New Levels of Transcription Control. *ChemBioChem* **2012**, *13*, 511−513.
(26) Yamazoe, S.; Liu, Q.; McQuade, L. E.; Deiters, A.; Chen, J. K. Sequential Gene Silencing Using Wavelength-Selective Caged Morpholino Oligonucleotides. *Angew. Chem., Int. Ed.* **2014**, *53*, 10114−10118.
(27) Pincock, J. A. Photochemistry of Arylmethyl Esters in Nucleophilic Solvents: Radical Pair and Ion Pair Intermediates. *Acc. Chem. Res.* **1997**, *30*, 43−49.
(28) Hansen, M. J.; Velema, W. A.; Lerch, M. M.; Szymanski, W.; Feringa, B. L. Wavelength-selective cleavage of photoprotecting groups: strategies and applications in dynamic systems. *Chem. Soc. Rev.* **2015**, *44*, 3358−3377.
(29) Kotzur, N.; Briand, B.; Beyermann, M.; Hagen, V. Wavelength-Selective Photoactivatable Protecting Groups for Thiols. *J. Am. Chem. Soc.* **2009**, *131*, 16927−16931.
(30) Mahmoodi, M. M.; Abate-Pella, D.; Pundsack, T. J.; Palsuledesai, C. C.; Goff, P. C.; Blank, D. A.; Distefano, M. D. Nitrodibenzofuran: A One- and Two-Photon Sensitive Protecting Group That Is Superior to Brominated Hydroxycoumarin for Thiol Caging in Peptides. *J. Am. Chem. Soc.* **2016**, *138*, 5848−5859.
(31) Mikkelsen, R. J. T.; Grier, K. E.; Mortensen, K. T.; Nielsen, T. E.; Qvortrup, K. Photolabile Linkers for Solid-Phase Synthesis. *ACS Comb. Sci.* **2018**, *20*, 377−399.
(32) Goguen, B. N.; Aemissegger, A.; Imperiali, B. Sequential Activation and Deactivation of Protein Function Using Spectrally Differentiated Caged Phosphoamino Acids. *J. Am. Chem. Soc.* **2011**, *133*, 11038−11041.
(33) Wong, P. T.; Tang, S.; Cannon, J.; Mukherjee, J.; Isham, D.; Gam, K.; Payne, M.; Yanik, S. A.; Baker, J. R.; Choi, S. K. A Thioacetal Photocage Designed for Dual Release: Application in the Quantitation of Therapeutic Release by Synchronous Reporter Decaging. *ChemBioChem* **2017**, *18*, 126−135.
(34) Momotake, A.; Lindegger, N.; Niggli, E.; Barsotti, R. J.; Ellis-Davies, G. C. R. The nitrodibenzofuran chromophore: a new caging group for ultra-efficient photolysis in living cells. *Nat. Methods* **2006**, *3*, 35−40.
(35) Givens, R. S.; Rubina, M.; Wirz, J. Applications of p-hydroxyphenacyl (pHP) and coumarin-4-ylmethyl photoremovable protecting groups. *Photochem. Photobiol. Sci.* **2012**, *11*, 472−488.
(36) Schönleber, R. O.; Bendig, J.; Hagen, V.; Giese, B. Rapid photolytic release of cytidine 5′-diphosphate from a coumarin derivative: a new tool for the investigation of ribonucleotide reductases. *Bioorg. Med. Chem.* **2002**, *10*, 97−101.
(37) Venkatesh, Y.; Nandi, S.; Shee, M.; Saha, B.; Anoop, A.; Pradeep Singh, N. D. Bis-Acetyl Carbazole: A Photoremovable Protecting Group for Sequential Release of Two Different Functional Groups and Its Application in Therapeutic Release. *Eur. J. Org. Chem.* **2017**, *2017*, 6121−6130.
(38) Venkatesh, Y.; Rajesh, Y.; Karthik, S.; Chetan, A. C.; Mandal, M.; Jana, A.; Singh, N. D. P. Photocaging of Single and Dual (Similar or Different) Carboxylic and Amino Acids by Acetyl Carbazole and its Application as Dual Drug Delivery in Cancer Therapy. *J. Org. Chem.* **2016**, *81*, 11168−11175.
(39) Fedoryak, O. D.; Dore, T. M. Brominated Hydroxyquinoline as a Photolabile Protecting Group with Sensitivity to Multiphoton Excitation. *Org. Lett.* **2002**, *4*, 3419−3422.
(40) Zhu, Y.; Pavlos, C. M.; Toscano, J. P.; Dore, T. M. 8-Bromo-7-hydroxyquinoline as a Photoremovable Protecting Group for Physiological Use: Mechanism and Scope. *J. Am. Chem. Soc.* **2006**, *128*, 4267−4276.
(41) Davis, M. J.; Kragor, C. H.; Reddie, K. G.; Wilson, H. C.; Zhu, Y.; Dore, T. M. Substituent Effects on the Sensitivity of a Quinoline Photoremovable Protecting Group to One- and Two-Photon Excitation. *J. Org. Chem.* **2009**, *74*, 1721−1729.
(42) Li, Y. M.; Shi, J.; Cai, R.; Chen, X.; Luo, Z. F.; Guo, Q. X. New quinoline-based caging groups synthesized for photo-regulation of aptamer activity. *J. Photochem. Photobiol., A* **2010**, *211*, 129−134.
(43) Fichte, M. A. H.; Weyel, X. M. M.; Junek, S.; Schäfer, F.; Herbivo, C.; Goeldner, M.; Specht, A.; Wachtveitl, J.; Heckel, A. Three-Dimensional Control of DNA Hybridization by Orthogonal Two-Color Two-Photon Uncaging. *Angew. Chem., Int. Ed.* **2016**, *55*, 8948−8952.
(44) Yoshida, S.; Hirose, S.; Iwamoto, M. Use of 4-bromomethyl-7-methoxycoumarin for derivatization of pyrimidine compounds in

https://dx.doi.org/10.1021/acs.joc.9b02617
J. Org. Chem. XXXX, XXX, XXX−XXX

serum analysed by high-performance liquid chromatography with fluorimetric detection. *J. Chromatogr. B: Biomed. Sci. Appl.* **1986**, *383*, 61−68.
(45) Kröck, L.; Heckel, A. Photoinduced Transcription by Using Temporarily Mismatched Caged Oligonucleotides. *Angew. Chem., Int. Ed.* **2005**, *44*, 471−473.
(46) Seio, K.; Ohno, Y.; Ohno, K.; Takeshita, L.; Kanamori, T.; Masaki, Y.; Sekine, M. Photo-controlled binding of MutS to photo-caged DNA duplexes incorporating 4- O -(2-nitrobenzyl) or 4- O -[2-(2-nitrophenyl)propyl]thymidine. *Bioorg. Med. Chem. Lett.* **2016**, *26*, 4861−4863.
(47) Hölz, K.; Hoi, J. K.; Schaudy, E.; Somoza, V.; Lietard, J.; Somoza, M. M. High-Efficiency Reverse (5′→3′) Synthesis of Complex DNA Microarrays. *Sci. Rep.* **2018**, *8*, 15099.
(48) Pickens, C. J.; Gee, K. R. Photolabile thymidine cleavable with a 532 nanometer laser. *Tetrahedron Lett.* **2011**, *52*, 4989−4991.
(49) San Miguel, V.; Bochet, C. G.; del Campo, A. Wavelength-Selective Caged Surfaces: How Many Functional Levels Are Possible? *J. Am. Chem. Soc.* **2011**, *133*, 5380−5388.
(50) Bourbon, P.; Peng, Q.; Ferraudi, G.; Stauffacher, C.; Wiest, O.; Helquist, P. Synthesis, Photophysical, Photochemical, and Computational Studies of Coumarin-Labeled Nicotinamide Derivatives. *J. Org. Chem.* **2012**, *77*, 2756−2762.
(51) Herzig, L.-M.; Elamri, I.; Schwalbe, H.; Wachtveitl, J. Light-induced antibiotic release from a coumarin-caged compound on the ultrafast timescale. *Phys. Chem. Chem. Phys.* **2017**, *19*, 14835−14844.
(52) Kim, Y. A.; Ramirez, D. M. C.; Costain, W. J.; Johnston, L. J.; Bittman, R. A new tool to assess ceramide bioactivity: 6-bromo-7-hydroxycoumarinyl-caged ceramide. *Chem. Commun.* **2011**, *47*, 9236−9238.
(53) Suzuki, A. Z.; Watanabe, T.; Kawamoto, M.; Nishiyama, K.; Yamashita, H.; Ishii, M.; Iwamura, M.; Furuta, T. Coumarin-4-ylmethoxycarbonyls as Phototriggers for Alcohols and Phenols. *Org. Lett.* **2003**, *5*, 4867−4870.
(54) Abate-Pella, D.; Zeliadt, N. A.; Ochocki, J. D.; Warmka, J. K.; Dore, T. M.; Blank, D. A.; Wattenberg, E. V.; Distefano, M. D. Photochemical Modulation of Ras-Mediated Signal Transduction Using Caged Farnesyltransferase Inhibitors: Activation by One- and Two-Photon Excitation. *ChemBioChem* **2012**, *13*, 1009−1016.
(55) Eckardt, T.; Hagen, V.; Schade, B.; Schmidt, R.; Schweitzer, C.; Bendig, J. Deactivation Behavior and Excited-State Properties of (Coumarin-4-yl)methyl Derivatives. 2. Photocleavage of Selected (Coumarin-4-yl)methyl-Caged Adenosine Cyclic 3′,5′-Monophosphates with Fluorescence Enhancement. *J. Org. Chem.* **2002**, *67*, 703−710.
(56) Hagen, V.; Dekowski, B.; Nache, V.; Schmidt, R.; Geißler, D.; Lorenz, D.; Eichhorst, J.; Keller, S.; Kaneko, H.; Benndorf, K.; Wiesner, B. Coumarinylmethyl Esters for Ultrafast Release of High Concentrations of Cyclic Nucleotides upon One- and Two-Photon Photolysis. *Angew. Chem., Int. Ed.* **2005**, *44*, 7887−7891.
(57) Lin, Q.; Bao, C.; Cheng, S.; Yang, Y.; Ji, W.; Zhu, L. Target-Activated Coumarin Phototriggers Specifically Switch on Fluorescence and Photocleavage upon Bonding to Thiol-Bearing Protein. *J. Am. Chem. Soc.* **2012**, *134*, 5052−5055.
(58) Choi, S. K.; Verma, M.; Silpe, J.; Moody, R. E.; Tang, K.; Hanson, J. J.; Baker, J. R., Jr A photochemical approach for controlled drug release in targeted drug delivery. *Bioorg. Med. Chem.* **2012**, *20*, 1281−1290.
(59) Galindo, F. The photochemical rearrangement of aromatic ethers. *J. Photochem. Photobiol., C* **2005**, *6*, 123−138.
(60) Schaal, J.; Kotzur, N.; Dekowski, B.; Quilitz, J.; Klimakow, M.; Wessig, P.; Hagen, V. A novel photorearrangement of (coumarin-4-yl)methyl phenyl ethers. *J. Photochem. Photobiol., A* **2009**, *208*, 171−179.
(61) Asad, N.; Deodato, D.; Lan, X.; Widegren, M. B.; Phillips, D. L.; Du, L.; Dore, T. M. Photochemical Activation of Tertiary Amines for Applications in Studying Cell Physiology. *J. Am. Chem. Soc.* **2017**, *139*, 12591−12600.
(62) Deodato, D.; Asad, N.; Dore, T. M. Photorearrangement of Quinoline-Protected Dialkylanilines and the Photorelease of Aniline-Containing Biological Effectors. *J. Org. Chem.* **2019**, *84*, 7342−7353.
(63) Amir, R. J.; Pessah, N.; Shamis, M.; Shabat, D. Self-Immolative Dendrimers. *Angew. Chem., Int. Ed.* **2003**, *42*, 4494−4499.
(64) Ito, K.; Nakajima, K. Selenium dioxide oxidation of alkylcoumarins and related methyl-substituted heteroaromatics. *J. Heterocycl. Chem.* **1988**, *25*, 511−515.
(65) Xu, Y.-Z.; Swann, P. F. A simple method for the solid phase synthesis of oligodeoxynucleotides containing O4-alkylthymine. *Nucleic Acids Res.* **1990**, *18*, 4061−4065.
(66) Sung, W. L. Chemical conversion of thymidine into 5-methyl-2′-deoxycytidine. *J. Chem. Soc., Chem. Commun.* **1981**, 1089a.
(67) Hatchard, C. G.; Parker, C. A. A New Sensitive Chemical Actinometer. II. Potassium Ferrioxalate as a Standard Chemical Actinometer. *Proc. R. Soc. London, Ser. A* **1956**, *235*, 518−536.
(68) Braslavsky, S. E. Glossary of terms used in photochemistry, 3rd edition (IUPAC Recommendations 2006). *Pure Appl. Chem.* **2007**, *79*, 293−465.
(69) Pincock, A. L.; Pincock, J. A.; Stefanova, R. Substituent Effects on the Rate Constants for the Photo-Claisen Rearrangement of Allyl Aryl Ethers. *J. Am. Chem. Soc.* **2002**, *124*, 9768−9778.
(70) Furuta, T.; Watanabe, T.; Tanabe, S.; Sakyo, J.; Matsuba, C. Phototriggers for Nucleobases with Improved Photochemical Properties. *Org. Lett.* **2007**, *9*, 4717−4720.
(71) Buhr, F.; Kohl-Landgraf, J.; tom Dieck, S.; Hanus, C.; Chatterjee, D.; Hegelein, A.; Schuman, E. M.; Wachtveitl, J.; Schwalbe, H. Design of Photocaged Puromycin for Nascent Polypeptide Release and Spatiotemporal Monitoring of Translation. *Angew. Chem., Int. Ed.* **2015**, *54*, 3717−3721.
(72) Gilbert, D.; Funk, K.; Dekowski, B.; Lechler, R.; Keller, S.; Möhrlen, F.; Frings, S.; Hagen, V. Caged Capsaicins: New Tools for the Examination of TRPV1 Channels in Somatosensory Neurons. *ChemBioChem* **2007**, *8*, 89−97.
(73) Kurata, M.; Hiyama, M.; Narimatsu, T.; Hazama, Y.; Ito, T.; Hayamizu, Y.; Qiu, X.; Winnik, F. M.; Akiyama, H. Synthesis and quantitative characterization of coumarin-caged D-luciferin. *J. Photochem. Photobiol., B* **2018**, *189*, 81−86.
(74) Weinrich, T.; Gränz, M.; Grünewald, C.; Prisner, T. F.; Göbel, M. W. Synthesis of a Cytidine Phosphoramidite with Protected Nitroxide Spin Label for EPR Experiments with RNA. *Eur. J. Org. Chem.* **2017**, *2017*, 491−496.

https://dx.doi.org/10.1021/acs.joc.9b02617
J. Org. Chem. XXXX, XXX, XXX−XXX